Available online at www.sciencedirect.com
ScienceDirect
Journal of Nuclear Materials 358 (2006) 111–128
journal of nuclear materials
www.elsevier.com/locate/jnucmat

Kinetics of thermal decomposition of sodium methoxide and ethoxide

K. Chandran [a], M. Kamruddin [b], P.K. Ajikumar [b], A. Gopalan [c], V. Ganesan [a,*]

[a] *Materials Chemistry Division, Indira Gandhi Centre for Atomic Research, Kalpakkam – 603 102, India*
[b] *Materials Science Division, Indira Gandhi Centre for Atomic Research, Kalpakkam – 603 102, India*
[c] *Department of Industrial Chemistry, Alagappa University, Karaikudi – 630 003, India*

Received 29 August 2005; accepted 9 July 2006

Abstract

Sodium methoxide and sodium ethoxide were synthesized. Their thermal decomposition and reaction kinetics were investigated under non-isothermal and isothermal conditions. Non-isothermal experiments were carried out at different linear heating rates. Kinetics of decomposition in each run was evaluated from the dynamic TGA and MS data obtained from thermogravimetric analyzer (TGA) coupled with mass spectrometer based evolved gas analyzer (EGA–MS). The activation energies derived from isothermal experiments by Arrhenius plot were 187.81 ± 11.22 and 150.84 ± 5.32 kJ mol^{-1} for sodium methoxide and sodium ethoxide, respectively, which agree well with the values from non-isothermal method. The evolved gases were found to be a mixture of saturated and unsaturated hydrocarbons. XRD, IR, AES, CHNS analyzer and volumetric estimation were employed to characterize the decomposition residue and identified as a mixture of sodium carbonate, sodium hydroxide and amorphous carbon. The probable mechanism and kinetics of decomposition of sodium alkoxides described in this paper are reported for the first time.

PACS: 81.70.P; 82.30.L; 61.10; 82.80

1. Introduction

Components in physical contact with liquid sodium in coolant circuits of Fast Reactors (FRs) get wetted with sodium on prolonged exposure and high temperature operation. These components need to be cleaned free of sodium when removed from coolant circuits for maintenance or replacement. As sodium reacts aggressively with moisture and oxygen present in air, careful handling and safe cleaning procedures are required to avoid any possible damage to men and material. Generally, lower members of aliphatic monohydric alcohols such as methanol, ethanol, denatured sprit and propanol have been used alone or as mixture of two or more of them as sodium cleaning agent while in certain cases long chain mono-hydric or di-hydric alcohols such as butyl cellosolve (2-butoxy ethanol) and ethyl

* Corresponding author. Tel.: +91 44 27480098; fax: +91 44 27480065.
E-mail address: ganesh@igcar.gov.in (V. Ganesan).

0022-3115/$ - see front matter © 2006 Elsevier B.V. All rights reserved.
doi:10.1016/j.jnucmat.2006.07.003

carbitol (di-ethylene glycol mono ethyl ether or 2,2′ ethoxy ethoxy ethanol) were used [1–16]. The runaway reaction leading to accident reported in literature when ethyl carbitol was used for sodium cleaning purpose was postulated to be due to the thermal instability of the reaction products of sodium and ethyl carbitol [2,5]. The present work was undertaken to study the thermal stability of sodium alkoxides namely sodium methoxide and sodium ethoxide. Pfeifer and Flora [17] have studied the decomposition of sodium methoxide and Blanchard et al. [18] have reported the decomposition of sodium ethoxide. The present study was mainly focused on kinetic analysis of sodium methoxide and ethoxide decomposition since there exists no data on activation energy of decomposition of these compounds.

2. Experimental

2.1. Preparation of compounds

Nuclear grade sodium (purity 99.5%) from Alkali Metals, India was further purified by vacuum distillation [19]. High Pressure Liquid Chromatography (HPLC) grade methanol (purity 99.8%) from Ranbaxy Fine Chemicals, India and absolute ethanol (purity 99.9%) from Hayman, UK were further purified by distillation [20] and used for preparation of sodium methoxide and sodium ethoxide. The reaction of sodium metal with alcohol to yield respective sodium alkoxide was performed under argon atmosphere using a vacuum tight glass vessel. The details of preparation and characterization of these alkoxides are described elsewhere [21]. Free flowing milky white powder of sodium alkoxide was obtained and stored in moisture free inert atmosphere glove box. The formation and purity of sodium alkoxides were confirmed by IR analysis, powder X-ray diffraction technique, followed by elemental analysis by Atomic Emission Spectrometer (AES) and Carbon Hydrogen Nitrogen Sulphur (CHNS) analyzer.

2.2. Equipment

2.2.1. UHV–TGA–MS

A high temperature TGA system (SETSYS 16/18, Setaram, France), with resolution of 0.04 μg was used in this study. For the purpose of evolved gas analysis this equipment was coupled to an all metal ultra high vacuum chamber pumped by a combination of a sputter ion pump, a titanium sublimation pump and backed by a turbo molecular pump. It operates at a base pressure of 1×10^{-10} mbar and between 5×10^{-9} and 2×10^{-8} mbar during gas analysis. This high vacuum level ensures low background, better sensitivity and lower detection limits for mass spectrometry measurements. This chamber houses a 1–300 amu (HAL 2C, Hiden, UK) quadrupole mass spectrometer with an electron impact ionization source having a partial pressure detection limit of 1×10^{-14} mbar, an inverted magnetron gauge and a spinning rotor viscosity gauge for absolute pressure measurement and calibration. The evolved gases, extracted very close to sample crucible at TGA, was fed to the measurement chamber in a controlled way through a variable leak valve for continuous analysis by mass spectrometer. The detailed description of the facility is given elsewhere [22].

2.3. TGA–MS measurements

Sodium alkoxides pellets of 4 mm diameter and 3–5 mm height were made from free flowing powder using a hand held press (PARR Instruments, USA) in a high purity, moisture free argon atmosphere glove box. For TGA–MS measurements the pellet was taken in a platinum crucible. Immediately after loading the sample, the TGA system was evacuated and filled with high purity argon gas twice to reduce the residual moisture level in the furnace atmosphere. Argon gas was allowed to flow through the furnace at the rate of 125 mL min^{-1} throughout the experiment. The measurements were carried out in both non-isothermal (heating rates 3, 5 and 10 K min^{-1} up to 700 K) and isothermal (623, 628, 633 and 638 K in the case of sodium methoxide and 573, 578, 583 and 593 K in the case of sodium ethoxide) heating modes. The sample weight change measured by TGA and the variation in concentration of product gases measured by mass spectrometer were continuously recorded as a function of time and temperature.

In isothermal experiments, the sample was heated at a faster manner to a predetermined temperature close to decomposition temperature with a heating rate of 25 K min^{-1} and held at that temperature till completion of decomposition. In these experiments sample weight changes were recorded as a function of time.

2.4. Characterization of residue

2.4.1. Elemental analysis

2.4.1.1. Analysis of carbon and hydrogen. About 10 mg of solid residues left behind after the decomposition of methoxide and ethoxide of sodium were loaded in tin crucibles of 3.5 mm dia. and 9 mm height inside an argon atmosphere glove box and sealed hermitically by crimping. Leak tightness of the crucible was ensured by observing absence of any change in sample weight monitored as a function of time over a period of 10 h in air at room temperature. These crucibles were loaded in CHNS elemental analyzer (Elementar Vario EL, Germany) for determination of carbon and hydrogen contents by combustion followed by thermal conductivity techniques. High purity sulfanilic acid, benzoic acid and mandelic acid (MERK, >99%), were used as standards. The error involved in the elemental analysis was found to be <1%. AR grade sodium

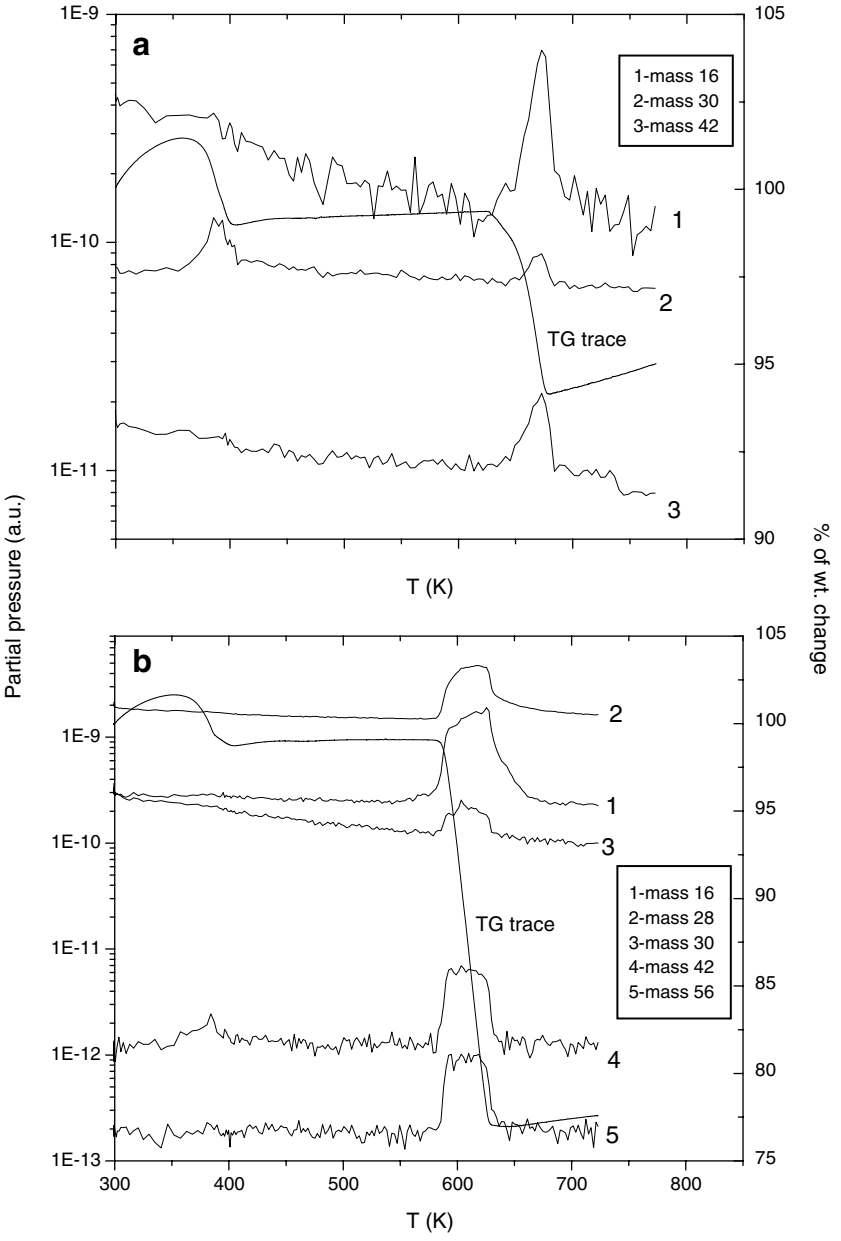

Fig. 1. Typical TGA–MS curve for decomposition of (a) sodium methoxide and (b) sodium ethoxide at a heating rate of 5 K min^{-1}.

benzoate of purity 99.0% (Samir Tech-Chem Industry, India), a sodium substituted compound, was also analyzed to cross-check the carbon and hydrogen contents with that of the sodium alkoxides residues.

2.4.1.2. Analysis of sodium in residue. Stock solutions were prepared by dissolving about 100 mg each of the decomposition residues of sodium methoxide and sodium ethoxide in dilute hydrochloric acid and distilled water. Necessary dilutions were made by taking aliquot from these stock solutions and used for sodium analysis using Atomic Absorption/Emission Spectrometer, (Model 751, Instrumental Laboratory Inc., USA) in emission mode. Calibration was carried out using sodium chloride standard solution in the concentration range of 1–10 $\mu g\ mL^{-1}$.

2.4.1.3. Solubility test. About 110–150 mg of the decomposition residue of sodium methoxide and sodium ethoxide were dissolved independently in distilled water, hydrochloric acid and in ether to study the solubility of the residue. Some insoluble black particles were observed in case of water and hydrochloric addition, which were analyzed by powder-XRD, IR and CHNS methods.

2.4.1.4. Analysis of sodium carbonate and sodium hydroxide. Presence of carbonate radical in residue was confirmed by standard lime water test. About 100 mg decomposition residues of sodium methoxide and sodium ethoxide were dissolved in distilled water and filtered to quantify sodium carbonate and sodium hydroxide. The filtrate was titrated against the standard hydrochloric acid using methyl orange or phenolphthalein as indicator to find the total alkalinity and sodium hydroxide alkalinity, respectively.

2.4.2. Infrared analysis

The decomposition residue of sodium methoxide was mixed with spectroscopic grade KBr powder and pelletized. The pellet was sandwiched between two ZnSe windows fitted in a leak tight sample holder to protect the sample from moisture. All these operations were carried out inside an argon atmosphere glove box. The IR spectrum of the sample thus prepared was recorded using a Fourier Transform Infrared spectrometer, (BOMEM MB100) in the range of 4000–400 cm^{-1} at 4 cm^{-1} resolution. Similar procedure was followed for recording IR spectra of sodium ethoxide decomposition residue and the insoluble portions of decomposition residues. To compare the spectral features of the residue, IR spectrum was recorded for GR grade sodium carbonate (purity 99.8%) from Sarabai M Chemicals, India.

2.4.3. X-ray diffraction analysis

X-ray diffractogram was recorded for the decomposition residues of sodium methoxide, sodium ethoxide and the black particles (insoluble in water and HCl) using a powder X-ray diffractometer (STOE, Germany) at room temperature with Cu Kα radiation. The samples were loaded in Lindemann glass capillaries sealed using paraffin wax in argon atmosphere glove box to protect against moisture. The X-ray powder diffraction patterns were recorded in the angular range of 5°–65° with a step size of 0.05°. The scan rate was 10 s per step.

3. Results and discussion

The IR spectra and XRD patterns of sodium methoxide and sodium ethoxide are presented elsewhere [21]. Absence of spectral features around 3500 and 1600 cm^{-1} region clearly shows that the methoxide and ethoxide of sodium prepared are free of alcohol and moisture. The XRD patterns of these compounds matched well with those reported in the literature [23,24] thereby confirming the formation as well as the purity of sodium methoxide and ethoxide used in the present study.

The TGA–MS spectra of decomposition of sodium alkoxides carried out at a heating rate of 5 $K\ min^{-1}$, giving the change in sample weight and intensity of gaseous products formed are shown in Fig. 1(a) and (b). The decomposition patterns obtained under other heating rates (3 and

Table 1
Elemental analysis results by CHNS analyzer and Atomic Emission Spectroscopy

Compound	Carbon (wt%)	Hydrogen (wt%)	Sodium (wt%)
Sodium methoxide residue	15.21 (14.71)	0.37 (0.98)	44.17 (45.07)
Sodium ethoxide residue	17.05 (17.41)	1.96 (0.97)	43.81 (44.50)

Theoretical composition is given in parenthesis and oxygen is not analyzed.

Table 2
Sodium content derived from sodium carbonate and sodium hydroxide (volumetric analysis) of the residues along with the insoluble content

Decomposition residue	Soluble content (wt%)			Insoluble content (wt%)		Sodium content (wt%)		
	Na_2CO_3	NaOH	Total	Calculated	Observed	From Na_2CO_3	From NaOH	Total
Sodium methoxide	52.31	40.32	92.63	7.37	7.25	22.70	23.18	45.88
Sodium ethoxide	50.01	40.80	90.81	9.20	8.00	21.70	23.46	45.16

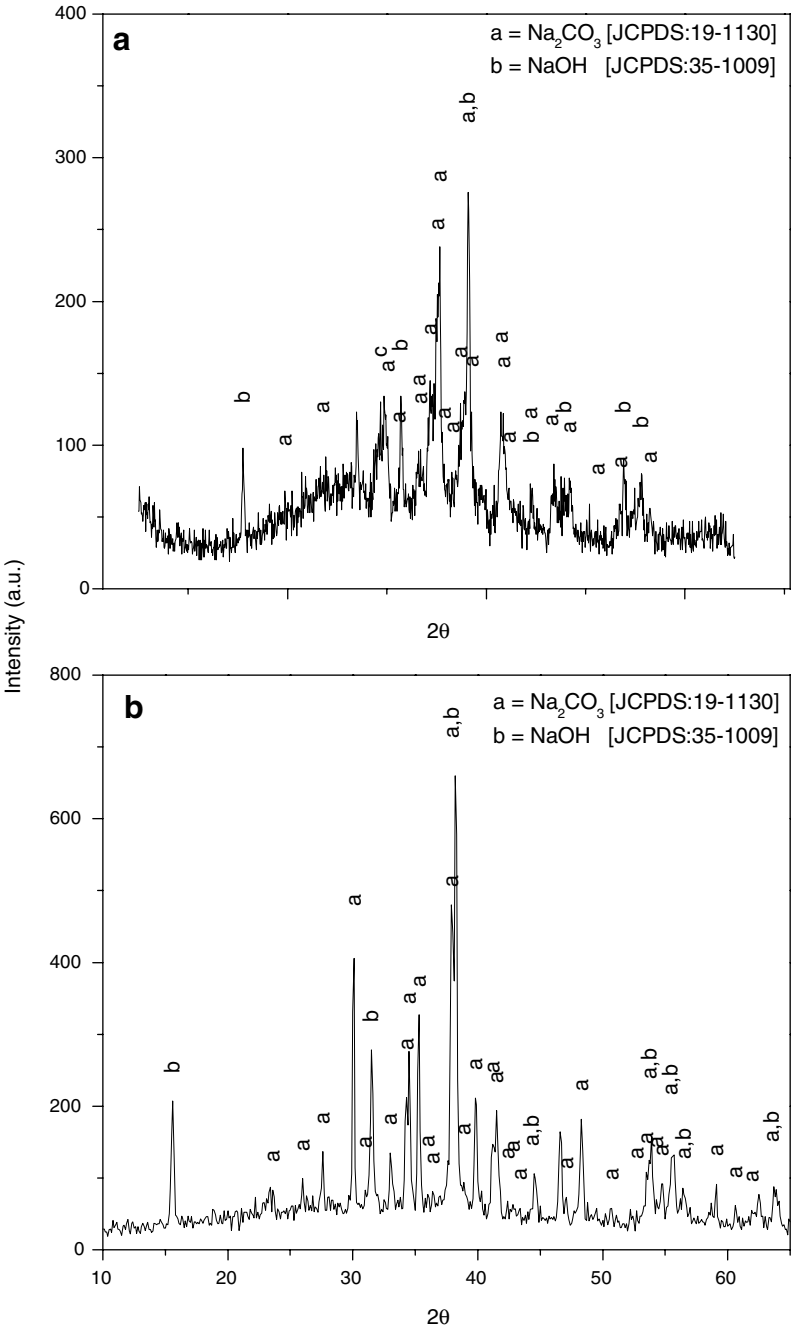

Fig. 2. XRD pattern for decomposition residues of (a) sodium methoxide and (b) sodium ethoxide.

10 K min^{-1}) are also similar except for the typical increase in the observed decomposition temperatures with increase in heating rate.

The initial weight gain in TG trace is due to the absorption of atmospheric moisture by the sample while loading. The first weight loss observed around 344 K is due to the evaporation of alcohol, which is formed by the reaction of sodium alkoxides with moisture picked up by the sample during loading into the instrument. This is confirmed by heating fresh compound of sodium methoxide and sodium ethoxide separately up to 450 K and subjecting the residue to X-ray and IR analysis. The XRD pattern and IR spectra obtained for the residue matched exactly with that of the pure compound.

The decomposition of sodium methoxide starts above 623 K (Fig. 1(a)). The gaseous products formed on decomposition were mainly methane (mass: 16) and minor quantities of ethane (mass: 30) and propylene (mass: 42). The solid residue was found to be a mixture of sodium carbonate, sodium hydroxide and amorphous carbon. However, it is to be noted that Pfeifer and Flora [17] have reported that the decomposition temperatures of sodium methoxide were 393 and 413 K with ethylene, water and sodium oxide as decomposition products.

The decomposition of sodium ethoxide is observed to start above 573 K (Fig. 1(b)) agreeing well with that reported by Blanchard et al. [18]. The gaseous products formed on decomposition were mainly methane (mass: 16) and ethylene (mass: 28) with minor quantities of ethane (mass: 30), propylene (mass: 42) and butylene (mass: 56). In this case also the solid residue was found to be a mixture of sodium carbonate, sodium hydroxide and amorphous carbon. However, in an earlier study on decomposition of sodium ethoxide [18], by collecting and condensing the evolved gases in liquid nitrogen and analysis by gas chromatography, the authors have reported the gaseous products to be mainly of ethylene and minor quantities of propane, heptane, ethanol and water. The authors have also stated that the non-condensable gas at liquid nitrogen temperature could be hydrogen or methane. The TG trace for decomposition of sodium ethoxide in their study indicated a slow and steady decomposition right from 273 K with a sharp weight change above 573 K which implied that the sodium ethoxide could contain some amount of ethanol and moisture that evaporated on heating. On cooling with liquid nitrogen, the evolved ethanol would also have condensed and reflected in the analysis. The authors have also mentioned the presence of nitrogen and water. The release of nitrogen from sodium ethoxide decomposition is unlikely and this also indicated that the ambient air could have condensed leading to contribution of nitrogen and water. However, in the present work, ethanol (mass: 46), water (mass: 18) and heptane (mass: 100) were not observed as product gases. The formation of higher alkene and the observed higher weight losses in the case of sodium ethoxide decomposition are due to the presence of an additional $–CH_2$ group. The weight losses observed for the methoxide and ethoxide of sodium were 6 and 24 wt%, respectively.

Carbon monoxide and ethylene having same molecular mass could be the possible product gases individually or together in the decomposition of

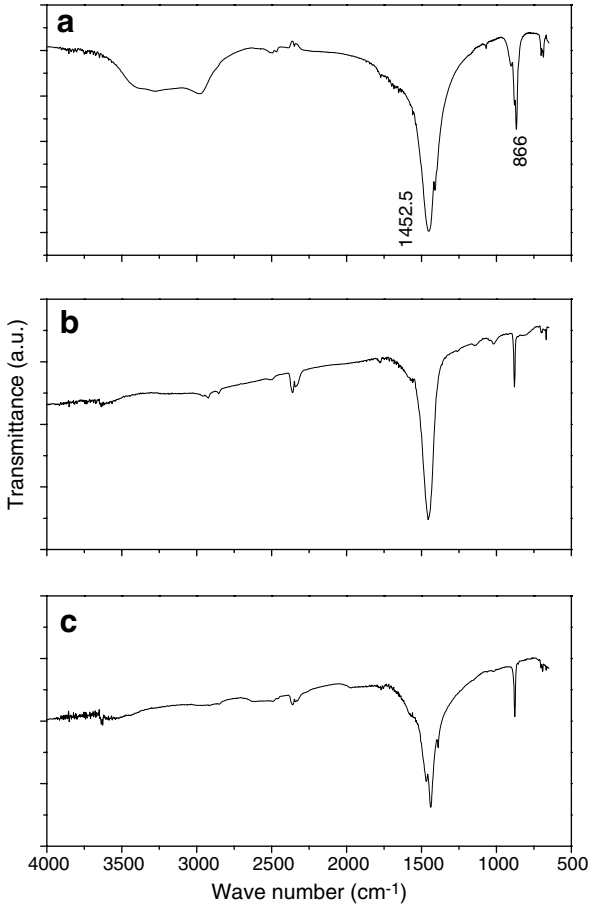

Fig. 3. IR spectra of (a) sodium carbonate, (b) decomposition residue of sodium methoxide and (c) decomposition residue of sodium ethoxide.

sodium ethoxide. However, their isobaric interference is overcome by using their respective finger print mass spectra and also by IR analysis of the gases. Thus it was confirmed that the mass 28 observed in the present case corresponds only to ethylene and not to carbon monoxide.

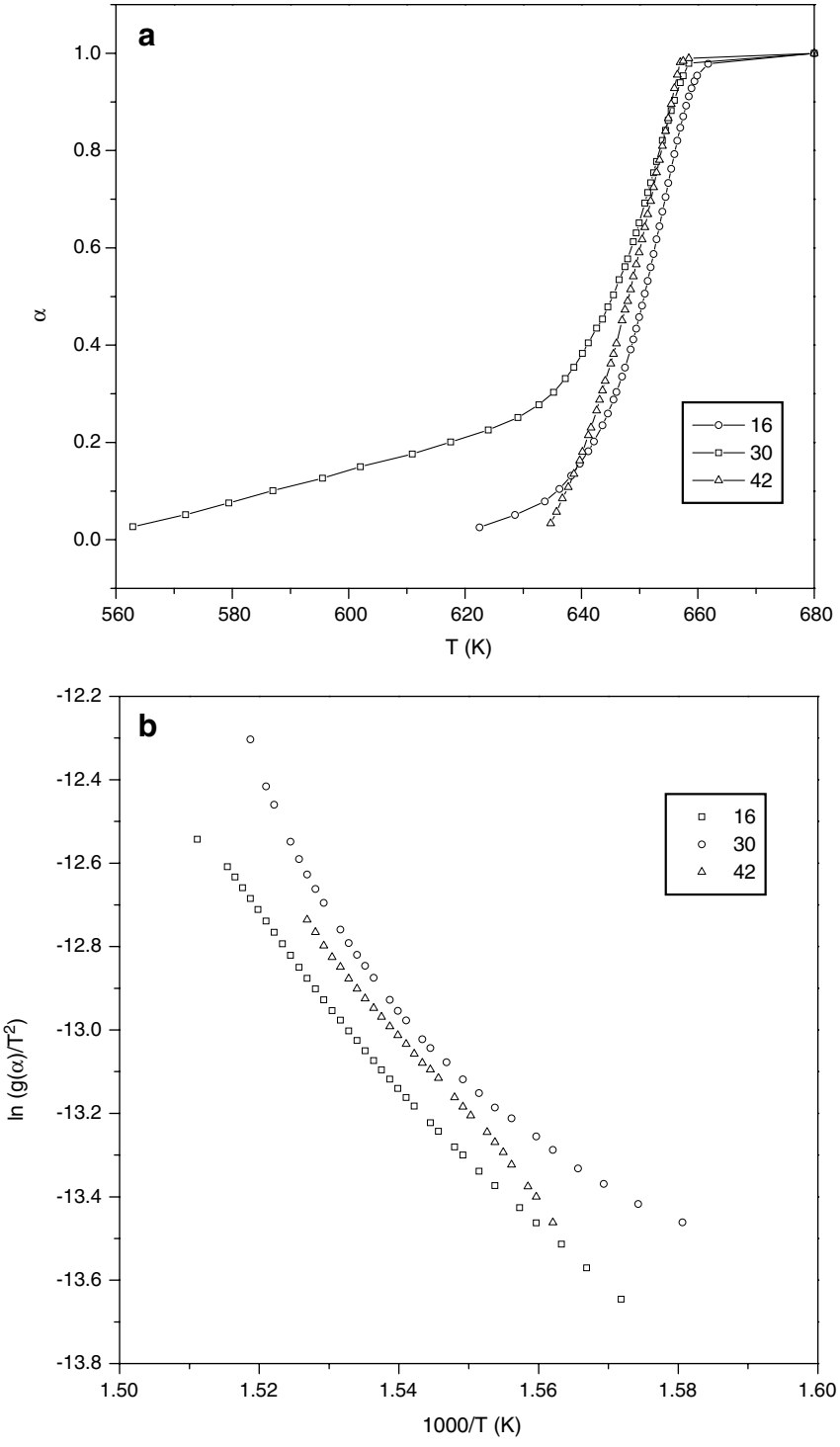

Fig. 4. (a) Plot of fraction formed against temperature and (b) $\ln(g(\alpha)/T^2)$ vs $1/T$ for the decomposition of sodium methoxide (heating rate: 5 K min^{-1}).

Sodium methoxide and sodium ethoxide on decomposition produce saturated and unsaturated gaseous hydrocarbons with black powdery residue. Various techniques such as AES, CHNS, volumetric and gravimetric analysis, IR analysis and XRD were used to characterize the solid residue.

The results of carbon, hydrogen and sodium analysis of the decomposition residue of sodium methoxide and ethoxide are given in Tables 1 and 2. It can

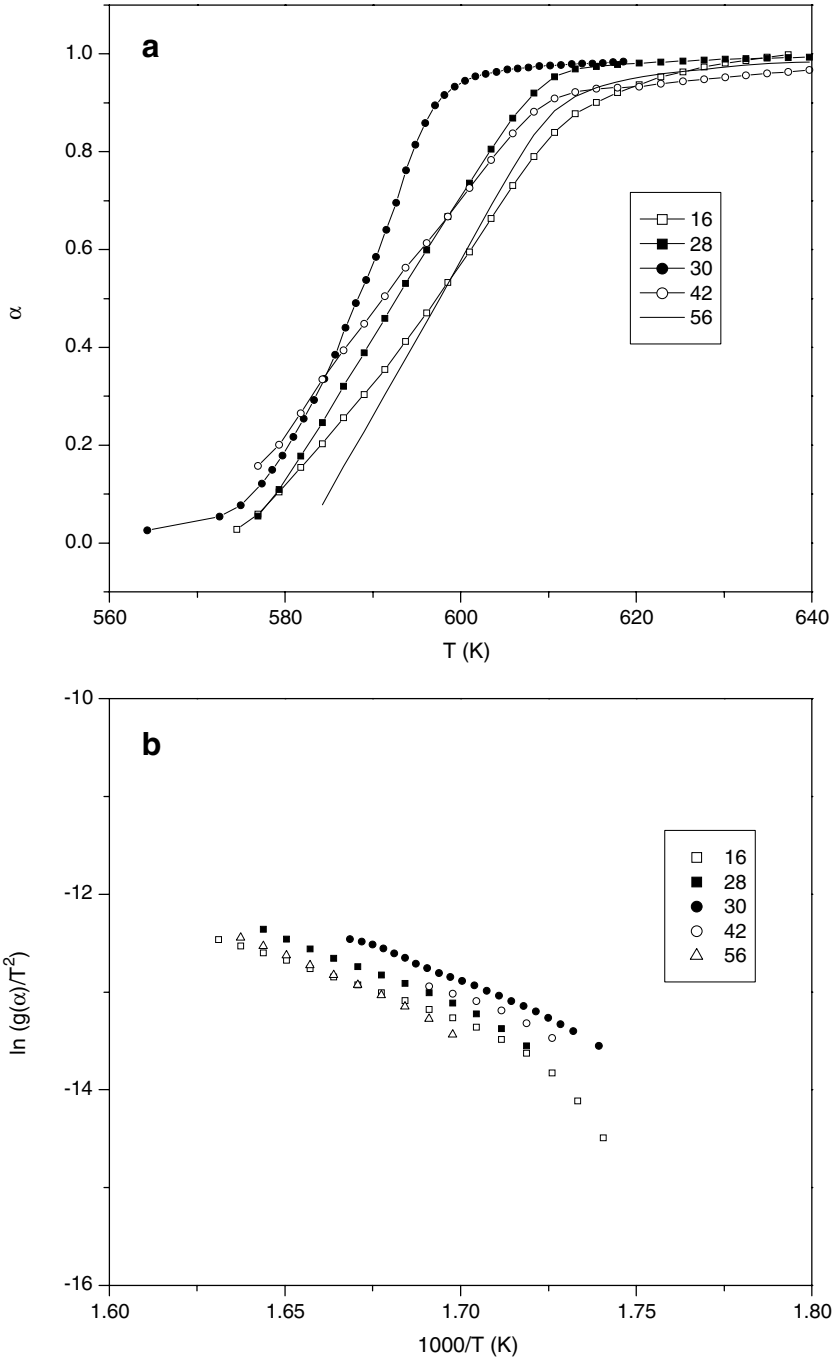

Fig. 5. (a) Plot of fraction formed against temperature and (b) $\ln(g(\alpha)/T^2)$ vs $1/T$ for the decomposition of sodium ethoxide (heating rate: 5 K min^{-1}).

be seen from Tables 1 and 2 that the residue contains carbon, hydrogen and sodium. The gaseous hydrocarbons formed on decomposition contain only carbon and hydrogen and hence, the residue should be species containing oxygen. Volumetric titration method was resorted to estimate the quantity of sodium carbonate and sodium hydroxide to account for oxygen and the results are given in Table 2. The total sodium content contributed by sodium carbonate and sodium hydroxide matches exactly with that of the total sodium content estimated by AES technique and confirms that the decomposition residue contain sodium carbonate and sodium hydroxide in the mole ratio of 1:2.

The weight percent of soluble and insoluble portions of the decomposition residues of sodium methoxide and sodium ethoxide in distilled water and in hydrochloric acid were same and are given in Table 2. It was clear that the weight percent of soluble portions of the solid residue were due to the sodium carbonate and sodium hydroxide. The measured weight percent of free carbon, the insoluble residue, was found to be slightly less compared to that calculated as complete retrieval of carbon particles from filter paper could not be achieved. The sum of carbon content contributed by sodium carbonate and free carbon has excellent agreement with that estimated by CHNS analyzer.

Addition of dilute hydrochloric acid to the decomposition residues of sodium methoxide and sodium ethoxide produced brisk effervescence indicating that the residues might contain carbonate. Subsequent limewater test confirmed that the residue contained sodium carbonate. As additional

Table 3
Calculated activation energy (E_a) and pre-exponential factor (A) under non-isothermal conditions from MS data

Compound	Product	Heating rate (K min^{-1})	Activation energy E_a (kJ mol^{-1})	Pre-exponential factor A (min^{-1})	Correlation coefficient	Standard deviation
Sodium methoxide	Methane		**164.54 ± 9.14**	**7.23×10^6**		
		3	155.89 ± 2.48	6.99×10^6	0.9957	0.03
		5	138.01 ± 5.25	1.03×10^5	0.9957	0.04
		10	124.12 ± 4.39	3.39×10^3	0.9981	0.03
	Ethane		**162.96 ± 3.47**	**4.48×10^6**		
		3	152.04 ± 7.13	4.31×10^6	0.9716	0.08
		5	140.17 ± 4.25	1.22×10^5	0.98	0.14
		10	122.70 ± 2.25	7.68×10^3	0.9529	0.15
	Propylene		**165.41 ± 6.22**	**2.91×10^7**		
		3	162.79 ± 1.31	2.79×10^7	0.9992	0.01
		5	152.81 ± 2.41	1.67×10^6	0.9995	0.01
		10	148.80 ± 7.17	6.92×10^5	0.9965	0.05
Sodium ethoxide	Methane		**140.34 ± 0.70**	**1.21×10^6**		
		3	133.60 ± 8.71	1.07×10^6	0.9695	0.14
		5	130.03 ± 7.29	2.33×10^5	0.9699	0.15
		10	118.76 ± 5.40	3.00×10^4	0.9959	0.06
	Ethylene		**139.50 ± 4.06**	**2.45×10^5**		
		3	124.78 ± 3.82	2.26×10^5	0.9953	0.04
		5	120.35 ± 1.58	1.49×10^4	0.9037	0.17
		10	95.58 ± 4.05	1.76×10^2	0.9926	0.06
	Ethane		**132.16 ± 1.95**	**6.49×10^5**		
		3	127.84 ± 2.03	5.62×10^5	0.9975	0.03
		5	122.38 ± 2.40	1.33×10^5	0.9969	0.04
		10	115.29 ± 1.53	4.19×10^3	0.9981	0.03
	Propylene		**144.41 ± 5.78**	**2.55×10^5**		
		3	123.93 ± 8.15	2.18×10^5	0.9915	0.29
		5	117.93 ± 4.74	5.55×10^4	0.9756	0.18
		10	83.47 ± 2.74	2.2×10^1	0.9953	0.04
	Butylene		**143.37 ± 0.99**	**4.45×10^5**		
		3	128.62 ± 3.69	3.98×10^5	0.9963	0.03
		5	117.48 ± 3.08	6.46×10^4	0.9943	0.06
		10	92.95 ± 2.83	1.30×10^2	0.9964	0.04

Values given in bold case are extrapolated ones.

confirmation, these residues were subjected to XRD and IR characterization. Powder X-ray diffraction patterns of the decomposition residues of sodium methoxide and sodium ethoxide are shown in Fig. 2(a) and (b). All the peaks were identified and found to match well with that of sodium carbonate and sodium hydroxide pattern reported [25,26]. The X-ray diffraction pattern of the water and HCl insoluble black particles exhibited only background spectra except a broad hump at 20°. This indicates that the insoluble residue is amorphous carbon.

Fig. 3(a)–(c) compares the IR spectrum of the residues obtained in the decomposition of sodium methoxide and sodium ethoxide with that of the commercially available sodium carbonate. The

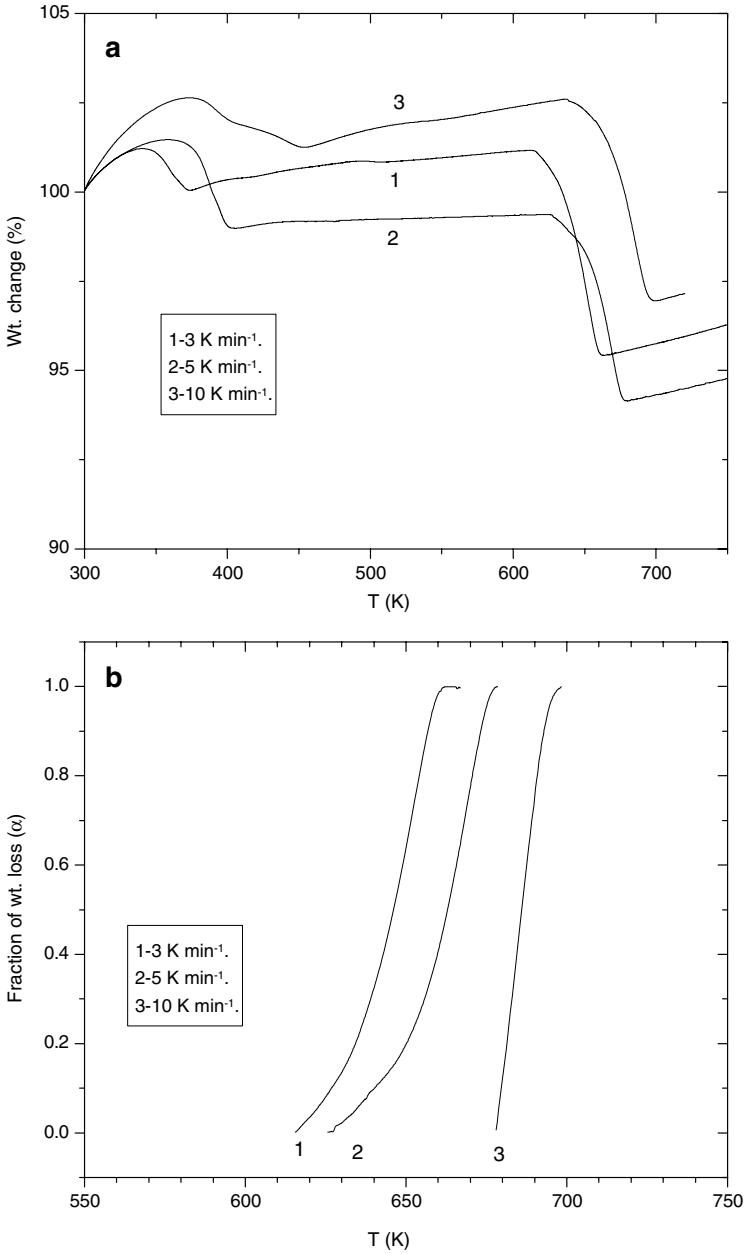

Fig. 6. (a) Plot of TG trace against temperature for decomposition of sodium methoxide and (b) plot of fraction of weight loss against temperature deduced from (a).

spectral features obtained for the residues around 1450 and 870 cm^{-1} match exactly with features of sodium carbonate recorded in the present work and also with that reported in literature [27]. This confirms that the residues contain sodium carbonate. The IR spectra of insoluble black particles did not show any spectral feature of C–C or C–H bonding. It is clear that the black particles were free of hydrocarbon.

From all these observations the possible decomposition reaction for the sodium alkoxide can be written as follows:

$$\mathrm{RONa} \rightarrow m\mathrm{Na_2CO_3} + x\mathrm{C} + 2m\mathrm{NaOH} + y\mathrm{C}_n\mathrm{H}_{2n+2} + z\mathrm{C}_n\mathrm{H}_{2n},$$

where m, x, y, and z are constants. n is the number of carbon atoms present in the hydrocarbon.

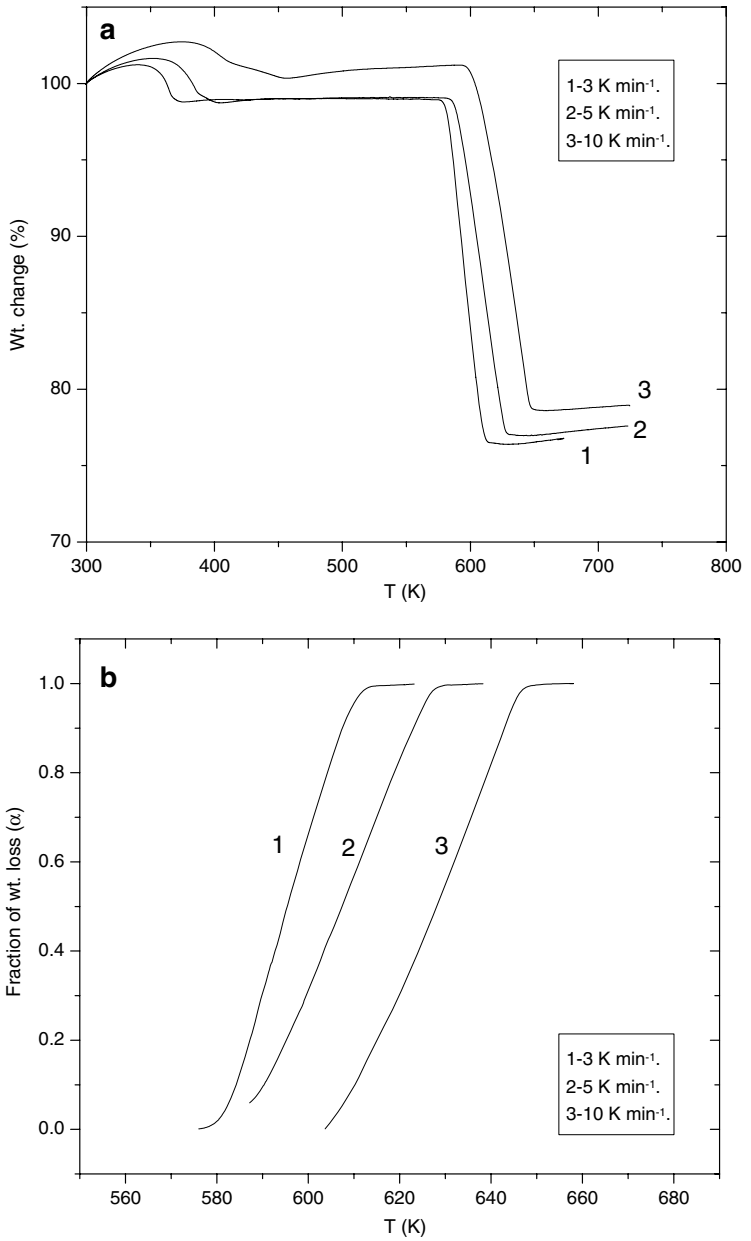

Fig. 7. (a) Plot of TG trace against temperature for decomposition of sodium ethoxide and (b) plot of fraction of weight loss against temperature deduced from (a).

$x = 1.5$ in the case of methoxide decomposition and 2 for ethoxide decomposition; R = methyl/ethyl group.

4. Kinetic analysis

Kinetic analysis of the TGA and MS data on the decomposition of sodium alkoxides was done to arrive at the possible mechanism of dissociation and association processes and to deduce the kinetic parameters. In the present study, kinetic parameters were evaluated by employing the model dependent method.

Since the reaction rate (r) is proportional to the amount of reactant at any time, t, it can be expressed by the following relation [28]:

$$r = \frac{d\alpha}{dt} = f(\alpha)k(T), \tag{1}$$

where α represents the extent of conversion of the reactant at time t (see Sections 4.1.1 and 4.1.2), $f(\alpha)$ is the conversion function which generally represents the mechanism of the reaction and k is the rate constant. The temperature dependence of the rate constant k, is generally expressed in Arrhenius form as

$$k(T) = A\exp(-E_a/RT), \tag{2}$$

where A is the pre-exponential factor, E_a the activation energy, R the universal gas constant and T the absolute temperature.

The non-isothermal rate equation can be represented as

$$\frac{d\alpha}{dT} = \frac{k(T)}{\beta} f(\alpha), \tag{3}$$

where β is the linear heating rate and $d\alpha/dT$ the temperature derivative of the extent of non-isothermal conversion. The general rate equation can be represented by combining Eq. (2) and (3) as

$$\frac{d\alpha}{dT} = \frac{A}{\beta}\exp(-E_a/RT)f(\alpha). \tag{4}$$

Rearrangement and integration of above expression within limit yields [29–33]

$$g(\alpha) = \int_0^{\alpha} \frac{d\alpha}{f(\alpha)} = \frac{A}{\beta}\int_0^{T} \exp(-E_a/RT)\,dT, \tag{5}$$

where the $g(\alpha)$ denotes the integral form of rate expression [34–38]. With necessary series solution and suitable approximations the integral reduces to

$$g(\alpha) = \frac{ART^2}{\beta E_a}\left[1 - \frac{2RT}{E_a}\right]\exp(-E_a/RT). \tag{6}$$

In logarithmic form this yields [39]

$$\ln\left[\frac{g(\alpha)}{T^2}\right] = \ln\left[\frac{AR}{\beta E_a}\left(1 - \frac{2RT}{E_a}\right)\right] - \frac{E_a}{RT}. \tag{7}$$

A plot of $\ln[g(\alpha)/T^2]$ vs $1/T$ yields a straight line for the appropriate $g(\alpha)$ function and from the intercept and slope, A and E_a, respectively, can be obtained.

4.1. Non-isothermal runs

4.1.1. Mass spectrometric data

In mass spectrometer applications, the conversion factor, α, is generally defined as

$$\alpha_{(T)} = \frac{Q_{(T)}}{Q_{(\text{Total})}} = \frac{A_{(T)}}{A_{(\text{Total})}},$$

Table 4
Calculated activation energy (E_a) and pre-exponential factor (A) under non-isothermal conditions from TGA data

Compound	Mechanism	Heating rate (K min^{-1})	Activation energy E_a (kJ mol^{-1})	Pre-exponential factor A (min^{-1})	Correlation coefficient	Standard deviation
Sodium methoxide	A2		**159.61 ± 0.5**	**1.11×10^7**		
		3	156.81 ± 0.23	9.63×10^6	0.9997	0.41
		5	154.23 ± 0.81	2.75×10^6	0.9969	0.03
		10	149.59 ± 0.6	5.95×10^5	0.9974	0.04
Sodium ethoxide	A2		**149.37 ± 9.47**	**1.03×10^7**		
		3	143.97 ± 0.40	9.89×10^6	0.9996	0.01
		5	127.75 ± 0.71	2.13×10^5	0.9943	0.05
		10	119.38 ± 0.31	1.78×10^4	0.9993	0.01

Values given in bold case are extrapolated ones.

where $Q_{(T)}$ and $Q_{(\mathrm{Total})}$ pertain to instantaneous and total quantities of gas which correspond to area under the release curves $A_{(T)}$ and $A_{(\mathrm{Total})}$, respectively. Detailed measurement of experimental $\alpha_{(T)}$ is described elsewhere [40].

Figs. 4(a) and 5(a) show the typical plot of fraction formed (α) vs temperature of various gaseous products formed on decomposition of sodium methoxide and ethoxide, respectively, at a heating rate of 5 K min^{-1}. Similar plots were also made

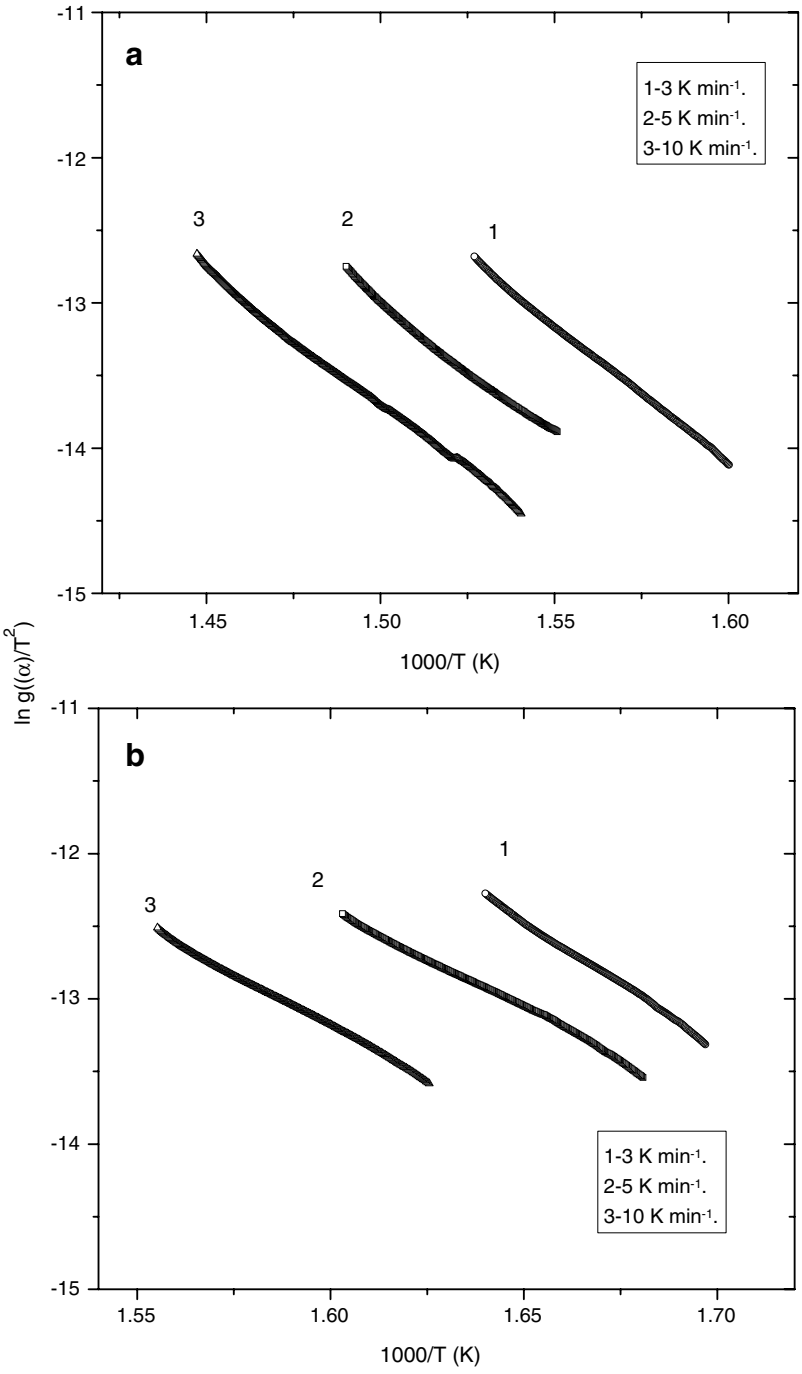

Fig. 8. Plot of $\ln(g(\alpha)/T^2)$ vs $1/T$ for (a) sodium methoxide and (b) sodium ethoxide.

for other heating rates. $\ln(g(\alpha)/T^2)$ vs reciprocal temperature were plotted and are shown in Figs. 4(b) and 5(b) for the decomposition of sodium methoxide and ethoxide, respectively. The best fit with high correlation coefficient and less standard deviation for various $g(\alpha)$ values was selected to represent the possible controlling mechanism and found to match with A2 Avrami–Erofe'ev nucleation and growth model, represented as $g(\alpha) = [-\ln(1-\alpha)]^{1/2}$. According to this model the rate of formation of a product formed during decomposition is mainly controlled by the advancement of a reactant-product interface (at which the actual chemical transformation occurs) into unchanged reactant [41]. This involves formation of a growth nuclei of the product and its growth given by the change in the geometry of its advancing interface into the reactant provided its availability is ensured [41]. The growth mechanism observed to control the decomposition of alkoxides suggests that the formation of growth nuclei is fast and the free energy of activation for the subsequent

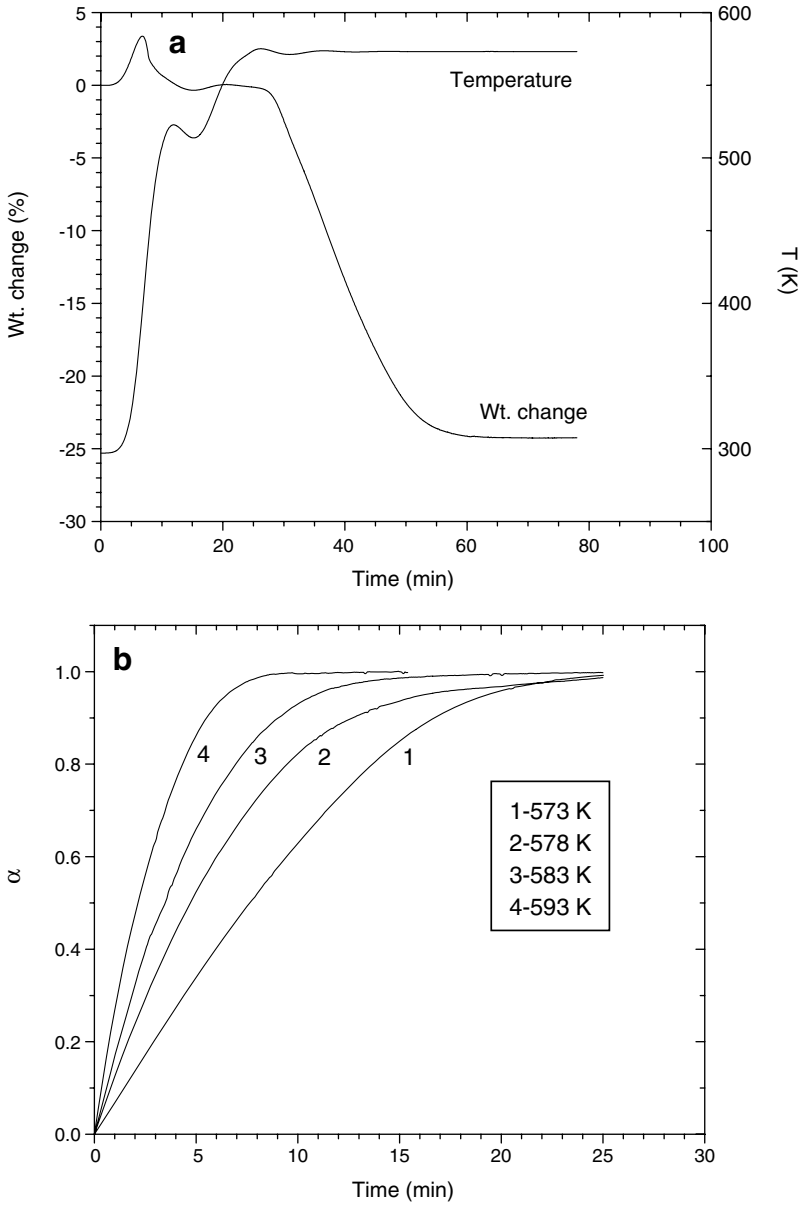

Fig. 9. Plot of sodium ethoxide decomposition (isothermal run) (a) Typical TGA data vs time and (b) α vs time.

growth process is more than that for the formation of growth nuclei. Thus the growth of the existing product domain controls the overall reaction than the formation of new nuclei [28]. When the growth of the nuclei is in the form of a two dimensional disk, then the control mechanism can be explained by A2 model. From the slope and intercept values, the activation energy and pre-exponential factor were calculated for different heating rates and are given in Table 3.

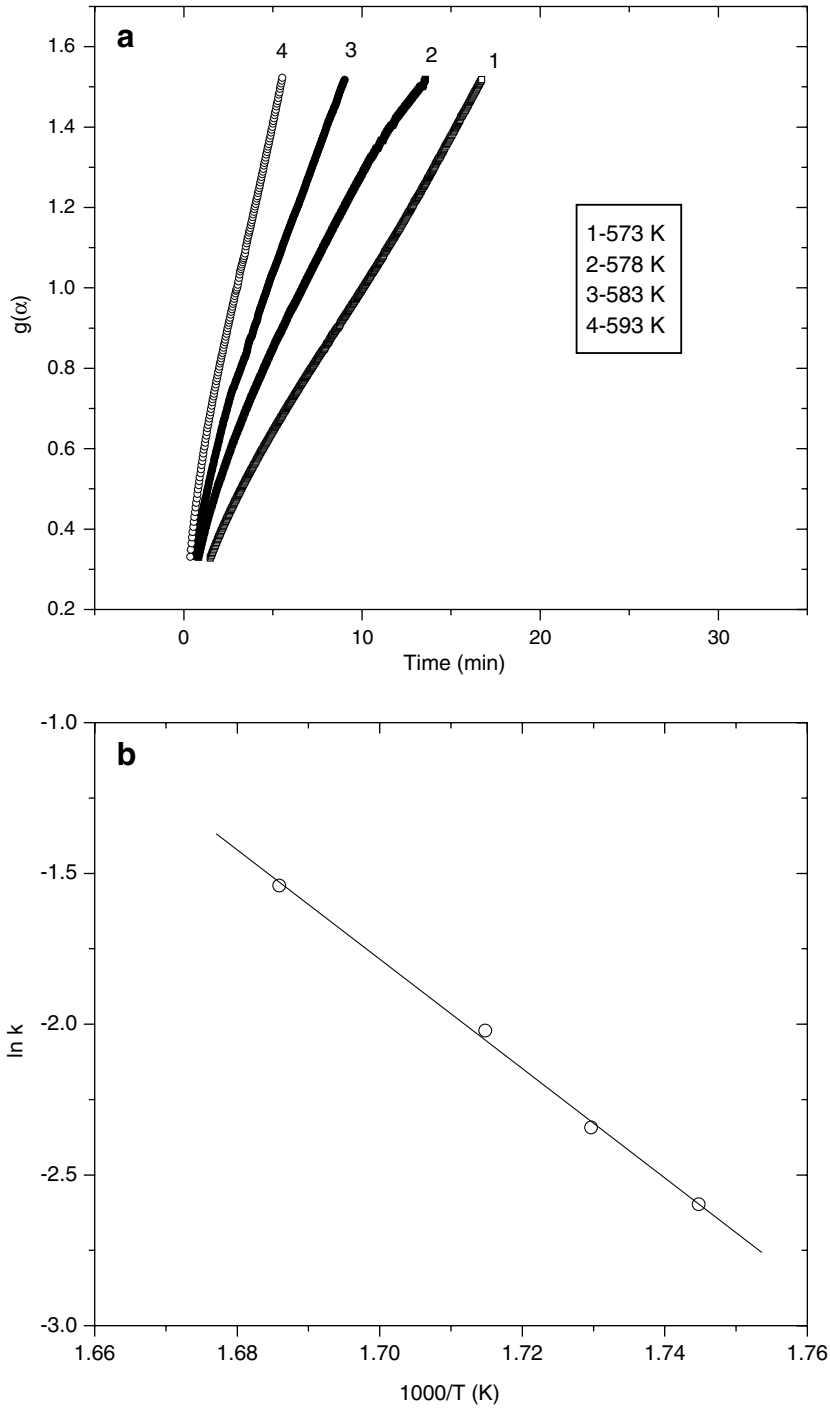

Fig. 10. Plot of sodium ethoxide decomposition (isothermal run) (a) $g(\alpha)$ vs time and (b) $\ln k$ vs $1/T$.

4.1.2. TGA data

In TG applications the conversion factor, α, is generally defined as

$$\alpha = \frac{(W_t - W_i)}{(W_f - W_i)},$$

where W is the weight of the sample and the subscripts i, t and f refer to the values at the beginning, at time t and at the end of the reaction, respectively.

Figs. 6(a) and 7(a) show the TGA plots of weight change as a function of absolute temperature for the decomposition of sodium methoxide and ethoxide at different heating rates. Figs. 6(b) and 7(b) show the corresponding plots of α vs T deduced from the above data. The plot of $\ln[g(\alpha)/T^2]$ vs $1/T$ gives a straight line when the correct $g(\alpha)$ function is used in the equation. As in the case of MS data, the $g(\alpha)$ function giving best fit with high correlation coefficient and low standard deviation was selected to represent the possible rate controlling mechanism. The corresponding activation energy and pre-exponential factor were then calculated from the slope and intercept of the above plots and are given in Table 4. Agreeing well with the MS data, the best fit for the decomposition of all the sodium alkoxides was obtained from A2 Avrami–Erofe'ev nucleation and growth model. Plots of $\ln[g(\alpha)/T^2]$ vs $1/T$ derived from TGA data are shown in Fig. 8(a) and (b).

Theoretically the activation energy of a process is expected not to change with change in heating rate. However, as it had been found and reported earlier [42–45] we have also observed a decrease in activation energy with increase in heating rate. The activation energy obtained from TG and MS data at different heating rates was plotted as a function of heating rate. A linear fit of this data is extrapolated and from its intercept the activation energy, which is equivalent to the activation energy arrived by isothermal experiments was calculated and shown in Tables 3 and 4. The close agreement in the extrapolated activation energy values obtained for different product gases highlight that they are formed simultaneously and from the same decomposition reaction, which is also seen from TGA–MS spectra (Fig. 1(a) and (b)).

4.2. Isothermal experiments

4.2.1. TG studies

Isothermal experiments were carried out to validate the reaction mechanisms and kinetic parameters deduced from non-isothermal experiments. The typical TGA plot giving the weight loss as a function of time for the decomposition of ethoxide at isothermal condition is shown in Fig. 9(a). The fractional extent 'α' derived from these isothermal decomposition runs of sodium ethoxide at different temperatures were shown in Fig. 9(b). Similar plots were also made for methoxide decomposition. The integral form of the isothermal kinetic equation is represented as

$$g(\alpha) = kt,$$

where k is the rate constant at a particular temperature and t the time. Various $g(\alpha)$ functions were plotted against time and the best fit with high correlation coefficient and less standard deviation was taken as the most appropriate mechanism of decomposition and shown in Fig. 10(a). As in non-isothermal experiments, Avrami–Erofe'ev A2 nucleation and growth model gives the best fit. The slope of the curve gives the rate constant of decomposition

Table 5
Values of the rate constants at different temperatures for the decomposition sodium alkoxides

Compound	Mechanism	Temperature (K)	Rate constant k (min^{-1})
Sodium methoxide	A2	623.15	7.7×10^{-2}
		628.15	9.6×10^{-2}
		633.15	1.3×10^{-1}
		638.15	1.79×10^{-1}
Sodium ethoxide	A2	573.15	7.45×10^{-2}
		578.15	9.61×10^{-2}
		583.15	1.33×10^{-1}
		593.15	2.14×10^{-1}

Table 6
Calculated activation energy (E_a) and pre-exponential factor (A) under isothermal conditions from TGA data

Compound	Mechanism	Activation energy E_a ($\mathrm{kJ\ mol}^{-1}$)	Pre-exponential factor A (min^{-1})	Correlation coefficient	Standard deviation
Sodium methoxide	A2	187.81 ± 11.22	4.15×10^{14}	0.9965	0.04
Sodium ethoxide	A2	150.84 ± 5.32	4.17×10^{12}	0.9988	0.03

reaction at a particular temperature. The rate constants obtained at different temperatures are given in Table 5. The plot of logarithm of rate constants obtained at different temperatures against reciprocal temperature is shown in Fig. 10(b). The activation energies for the decomposition of sodium methoxide and ethoxide were calculated from the slope of these plots using the Arrhenius equation and are given in Table 6.

The activation energies derived from non-isothermal experiments by both TGA and MS techniques were in good agreement with those calculated from isothermal runs. This confirms the validity of the reaction mechanism deduced for the decomposition of sodium methoxide and sodium ethoxide.

5. Conclusions

Pure sodium methoxide and sodium ethoxide were prepared and their decomposition is thoroughly investigated. Thermal decomposition of sodium methoxide and ethoxide starts above 623 and 573 K, respectively.

All the solid and gaseous decomposition products of sodium methoxide and sodium ethoxide were identified and reported for the first time. Solid residues of both contain sodium carbonate, sodium hydroxide and free carbon. The mole ratio of sodium carbonate and sodium hydroxide is 1:2. The gaseous products are mainly methane with minor quantities of ethane and propylene in the case of sodium methoxide decomposition. Methane and ethylene were the major constituents with ethane, propylene and butylene as minor constituents of gases formed in the case of sodium ethoxide decomposition.

The decomposition temperature is well above the boiling point of methanol and ethanol and the melting point of sodium (normally sodium cleaning carried out below the melting point of sodium). Hence, this study demonstrates that methanol and ethanol can safely be used for sodium cleaning purposes. Even any untoward temperature raise-up to 550 and 600 K during sodium cleaning process due to exothermic reaction in an accidental condition would not lead to any thermal decomposition of the reaction products.

The activation energies of decomposition reactions of sodium methoxide and sodium ethoxide are found to be in the range of 150–180 kJ mol^{-1} and were reported for the first time.

The activation energy calculated for the decomposition of sodium methoxide and sodium ethoxide by different methods and techniques were found to be consistent. This indicates that the activation energy of decomposition is dependent on process and independent of the nature of method namely non-isothermal or isothermal method as well as the TGA or MS technique.

Acknowledgements

The authors are grateful to Dr G. Periaswami, Head, Materials Chemistry Division, IGCAR for his constant encouragement throughout the course of the study and useful suggestions during the preparation of this paper. They thank Dr A.K. Tyagi, Materials Science Division, IGCAR for extending the experimental facility. The authors thank Dr K.S. Viswanathan and Dr K. Sankaran for their help in recording IR spectra and discussions during the course of this work and Dr R. Nithya for X-ray powder diffraction analysis. Thanks are also due to Mr C.V.S. Bramananda Rao for carrying out carbon and hydrogen estimation and to Mr A. Thriuvengadasami for help in analysis of sodium alkoxides using AES.

References

[1] J.G. Asquith, O.P. Steele, F.H. Welch, Sodium removal technology – the alcohol process, in: International Conference on Liquid Metal Technology in Energy Production, Champion, Pennsylvania, May 1976, p. 548.
[2] K.Ch. Stade, Operating experience in cleaning sodium-wetted components at the KNK nuclear power plant, IAEA/IWGFR Specialist Meeting on Sodium Removal and Decontamination, Richland, Washington, USA, February 1978, p. 1. Report IWGFR-23.
[3] E. Buscher, W. Haubold, W. Jansing, G. Kirchner, Sodium removal of fuel elements by vacuum distillation, IAEA/IWGFR Specialist Meeting on Sodium Removal and Decontamination, Richland, Washington, USA, February 1978, p. 38.
[4] B. De Luca, C. Grasso, M. Spadoni, Cleaning of small components of complex geometry by means of the sodium–alcohol reaction, IAEA/IWGFR Specialist Meeting on Sodium Removal and Decontamination, Richland, Washington, USA, February 1978, p. 139.
[5] R. Mukaibo, Y. Matsuno, I. Sato, Y. Yoneda, H. Sato, Sodium removal from the grapples of the fuel handling facility of JOYO, IAEA/IWGFR Specialist Meeting on Sodium Removal and Decontamination, Richland, Washington, USA, February 1978, p. 63.
[6] D.M. Donaldson, J.A. Bray, UK Fast Reactor Components – Sodium removal decontamination and requalification, IAEA/IWGFR Specialist Meeting on Sodium Removal and Decontamination, Richland, Washington, USA, February 1978, p. 110.

[7] O.P. Steele, W.F. Brehm, Summary of sodium removal and decontamination programmes in the USA, IAEA/IWGFR Specialist Meeting on Sodium Removal and Decontamination, Richland, Washington, USA, February 1978, p. 151.
[8] F.H. Welch, O.P. Steele, Non-aqueous removal of sodium from reactor components, IAEA/IWGFR Specialist Meeting on Sodium Removal and Decontamination, Richland, Washington, USA, February 1978, p. 173.
[9] R. Caponetti, M. Diamanti, M. Iacovelli, Sodium removal and technology at Casaccia CRE, in: Third International Conference on Liquid Metal Engineering and Technology, Oxford, vol. 2, April 1984, p. 141. The British Nuclear Energy Society, London, 1984.
[10] R. Caponetti, J. Nucl. Tech. 70 (1985) 408.
[11] Y. Waimei, D. Dejun, G. Huanfang, H. Shunzhang, Z. Shuxia, S. Fenyang, Y. Zhongmin, X. Yungxing, Some techniques for sodium removal in CIAE, IAEA/IWGFR – Technical Committee Meeting on Sodium Removal and Disposal from LMFRs in Normal Operation and in the Frame Work of Decommissioning, November 1997, Aix-en-Provence, France. Report IWGFR-98.
[12] P. Marmonier, J. Del Negro Cea, Information about the accident occurred near RAPSODIE, IAEA/IWGFR – Technical Committee Meeting on Sodium Removal and Disposal from LMFRs in Normal Operation and in the Frame Work of Decommissioning, November 1997.
[13] J. Minges, W. Cherdron, W. Schutz, Short report of an accident during sodium cleanup with ethyl carbitol in a storage tank of a research facility, IAEA/IWGFR – Technical Committee Meeting on Sodium Removal and Disposal from LMFRs in Normal Operation and in the Frame Work of Decommissioning, November 1997.
[14] D. Jambunathan, M.S. Rao, V.S. Krishnamachari, K.V. Kasiviswanathan, M. Rajan, Experience on sodium removal from FBTR components in its operating phase, IAEA/IWGFR – Technical Committee Meeting on Sodium Removal and Disposal from LMFRs in Normal Operation and in the Frame Work of Decommissioning, November 1997.
[15] K.K. Rajan, K. Grumoorthy, M. Rajan, R.D. Kale, Sodium cleaning and disposal methods in experimental facilities, IAEA/IWGFR – Technical Committee Meeting on Sodium Removal and Disposal from LMFRs in Normal Operation and in the Frame Work of Decommissioning, November 1997.
[16] S. Nakai, S. Yamamoto, M. Akai, T. Yatabe, Sodium removal by alcohol process, IAEA/IWGFR – Technical Committee Meeting on Sodium Removal and Disposal from LMFRs in Normal Operation and in the Frame Work of Decommissioning, November 1997.
[17] Gyulac Pfeifer, Terez Flora, Magy. Kem. Foly. 71 (8) (1965) 343.
[18] J.M. Blanchard, J. Bousquet, P. Claudy, J.M. Letoffe, J. Therm. Anal. 9 (1976) 191.
[19] V. Ganesan, D. Krishnamoorthy, N.P. Bhat, Determination of Oxygen in Sodium by the Vacuum Distillation Method, IGCAR Report IGC-87, 1986.
[20] B.S. Furniss, A.J. Hannaford, V. Rogers, P.W.G. Smith, A.R. Tatchell (Eds.), Vogel's Text book of Practical Organic Chemistry Including Qualitative Organic Analysis, 4th Ed., The English Language Book Society and Longman Group, London, 1980.
[21] K. Chandran, R. Nithya, K. Sankaran, A. Gopalan, V. Ganesan, Synthesis and characterization of sodium alkoxides, Bull. Mater. Sci. 29 (2) (2006) 173.
[22] M. Kamruddin, P.K. Ajikumar, S. Dash, A.K. Tyagi, Baldev Raj, Bull. Mater. Sci. 26 (4) (2003) 449.
[23] JCPDS – International Centre for Diffraction Data, PDF-2 database 1999, File 19-1876.
[24] JCPDS – International Centre for Diffraction Data, PDF-2 database 1999, File 19-1877.
[25] JCPDS – International Centre for Diffraction Data, PDF-2 database 1999, File 19-1130.
[26] JCPDS – International Centre for Diffraction Data, PDF-2 database 1999, File 35-1009.
[27] R.A. Nyquist, R.O. Kagel, Infrared Spectra of Inorganic Compounds, Academic Press, New York, 1971.
[28] C.H. Bamford, C.F.H. Tipper, Comprehensive Chemical Kinetics, vol. 22, Elsevier, Amsterdam, 1980.
[29] J.H. Sharp, G.W. Brindley, B.N.N. Achar, J. Am. Ceram. Soc. 49 (1966) 379.
[30] D. Dollimore, T.A. Evans, Y.F. Lee, F.W. Wilburn, Thermochim. Acta 188 (1991) 77.
[31] A.R. Salvador, E.G. Calvo, Thermochim. Acta 255 (1995) 155.
[32] J. Sestak, V. Satava, W.W. Wentlandt, Thermochim. Acta 7 (1973) 447.
[33] J. Zsako, J. Phys. Chem. 72 (1968) 2406.
[34] A. Finch, P.W.M. Jacob, F.C. Tompkins, J. Chem. Soc. (1954) 2053.
[35] M. Avrami, J. Chem. Phys. 7 (1939) 1103;
M. Avrami, J. Chem. Phys. 8 (1940) 212;
M. Avrami, J. Chem. Phys. 9 (1941) 177.
[36] E.G. Prout, F.C. Tompkins, Trans. Faraday Soc. 40 (1944) 488.
[37] W. Jander, Z. Anorg. Allg. Chem. 163 (1927) 1.
[38] A.M. Ginstling, B.I. Brounshtein, Zh. Prikl. Khim. 23 (1950) 131.
[39] A.N. Coats, J.P. Redfern, Nature 201 (1964) 68.
[40] S. Dash, M. Kamruddin, S. Bera, P.K. Ajikumar, A.K. Tyagi, S.V. Narasimhan, Baldev Raj, J. Nucl. Mater. 264 (1999) 271.
[41] A.K. Galwey, M.E. Brown, J. Therm. Anal. Cal. 60 (2000) 863.
[42] E. Urbanvici, E. Segal, Thermochim. Acta 107 (1986) 359.
[43] S.B. Kanungo, S.K. Mishra, Thermochim. Acta 241 (1994) 171.
[44] P.K. Heda, D. Dollimore, K.S. Alexander, D. Chen, E. Law, P. Bicknell, Thermochim. Acta 255 (1995) 255.
[45] Kitheri Joseph, R. Sridharan, T. Gnanasekaran, J. Nucl. Mater. 281 (2000) 129.